nature geoscience

LETTERS

PUBLISHED ONLINE: 25 OCTOBER 2009 | DOI: 10.1038/NGEO668

Warm and wet conditions in the Arctic region during Eocene Thermal Maximum 2

Appy Sluijs[1]*, Stefan Schouten[2], Timme H. Donders[1†], Petra L. Schoon[2], Ursula Röhl[3], Gert-Jan Reichart[4], Francesca Sangiorgi[1,2], Jung-Hyun Kim[2], Jaap S. Sinninghe Damsté[2,4] and Henk Brinkhuis[1]

Several episodes of abrupt and transient warming, each lasting between 50,000 and 200,000 years, punctuated the long-term warming during the Late Palaeocene and Early Eocene (58 to 51 Myr ago) epochs[1,2]. These hyperthermal events, such as the Eocene Thermal Maximum 2 (ETM2) that took place about 53.5 Myr ago[2], are associated with rapid increases in atmospheric CO_2 content. However, the impacts of most events are documented only locally[3,4]. Here we show, on the basis of estimates from the TEX'_{86} proxy, that sea surface temperatures rose by 3–5 °C in the Arctic Ocean during the ETM2. Dinoflagellate fossils demonstrate a concomitant freshening and eutrophication of surface waters, which resulted in euxinia in the photic zone. The presence of palm pollen implies[5] that coldest month mean temperatures over the Arctic land masses were no less than 8 °C, in contradiction of model simulations that suggest hyperthermal winter temperatures were below freezing[6]. In light of our reconstructed temperature and hydrologic trends, we conclude that the temperature and hydrographic responses to abruptly increased atmospheric CO_2 concentrations were similar for the ETM2 and the better-described Palaeocene–Eocene Thermal Maximum[7,8], 55.5 Myr ago.

At the onset of Eocene Thermal Maximum 2 (ETM2), the stable isotopic composition of sedimentary carbon ($\delta^{13}C$) shows a >1.5‰ negative excursion, interpreted as a geologically rapid injection of ^{13}C-depleted carbon into the ocean–atmosphere system[2,4,9]. A marked calcium carbonate dissolution horizon in deep-sea sediments reflects ocean acidification resulting from this carbon input[2,3]. Evidence for surface warming during ETM2 is, however, available only from the subtropical southeastern Atlantic Ocean, where a ~0.8‰ negative oxygen isotope excursion in calcite of surface-dwelling foraminifers was interpreted as a ~3 °C warming[2]. Hence, it remains uncertain whether ETM2 was associated with warming on a global scale and whether climate response was similar to the well-studied Palaeocene–Eocene Thermal Maximum (PETM).

Uppermost Palaeocene to Lower Eocene sediments were recovered from the Lomonosov Ridge, Arctic Ocean, at ~85° N palaeolatitude, during Integrated Ocean Drilling Program Expedition 302 (Supplementary Fig. S1). This ridge represents a fragment of continental crust that rifted from the Eurasian margin during the latest Palaeocene[10]. Upper Palaeocene and Lower Eocene sediments in Hole 4A consist of organic-rich, often laminated siliciclastic mudstones, barren of calcareous and siliceous microfossils but rich in assemblages of organic-walled dinoflagellate cysts (dinocysts), pollen and spores, and terrestrial and marine biomarkers[7,8,11–14]. High abundances of terrestrial components indicate that the drill site was located close to land[8] and the water depth was probably approximately 200 m (ref. 15). Recent studies have identified ETM2 in Core 27X of Hole 4A, ~20 m above the well-studied[7,8,11] PETM, on the basis of a negative carbon isotope excursion (CIE) in total organic carbon (TOC) and dinocyst biostratigraphy[8,12].

We generated a high-resolution $\delta^{13}C_{TOC}$ record across Core 27X to refine the position of the CIE associated with ETM2. This record shows a prominent ~3.5‰ drop between 368.94 and 368.79 m composite depth below sea floor (mcd) and a subsequent gradual recovery to background values at ~368.2 mcd (Fig. 1). Slightly above, at ~368.0 mcd, another ~2‰ negative step is recorded that potentially corresponds to the H2 carbon isotope event[9], which is ~100 kyr younger than ETM2 (ref. 2). A sedimentological break, however, separates this interval from ETM2, implying that the sediments could be younger than H2, but dinocyst biostratigraphy tentatively suggests an age close to H2 (Supplementary Information).

Dinocyst assemblages between 371 mcd and ETM2 are dominated by marine species (Fig. 1), globally known from shallow open-marine Lower Eocene settings, and assemblages are particularly similar to those from the Early Eocene of the North Sea (Supplementary Information). However, during ETM2, representatives of *Senegalinium* and *Cerodinium* that reflect dinoflagellates that tolerated low surface water salinities[16] and required nutrient-rich conditions[17], dominate assemblages, whereas the open-marine taxa completely disappear (Fig. 1). This pattern indicates a significant freshening and eutrophication of Arctic surface waters during ETM2. A doubling in relative abundances of terrestrial palynomorphs during ETM2 (Fig. 1) indicates that this was probably associated with an increase in Arctic precipitation and river runoff.

The occurrence of laminated sediments and the absence of organic benthic foraminiferal linings, which are regularly present between 371 and 368.9 mcd, suggest that bottom waters on Lomonosov Ridge became anoxic during ETM2. Concomitant with the highest abundances of freshwater-tolerant dinoflagellates within ETM2 and the CIE at ~368.0 mcd, sulphur-bound isorenieratane, a derivative of the carotenoid isorenieratene, is recorded (Fig. 1).

[1]Palaeoecology, Institute of Environmental Biology, Utrecht University, Laboratory of Palaeobotany and Palynology, Budapestlaan 4, 3584 CD Utrecht, The Netherlands, [2]NIOZ Royal Netherlands Institute for Sea Research, Department of Marine Organic Biogeochemistry, PO Box 59, 1790 AB, Den Burg, Texel, The Netherlands, [3]MARUM—Center for Marine Environmental Sciences, Bremen University, Leobener Strasse, 28359 Bremen, Germany, [4]Department of Earth Sciences, Utrecht University, Budapestlaan 4, 3584 CD Utrecht, The Netherlands. [†]Present address: TNO Geological Survey of the Netherlands, PO Box 80015, 3508 TA, Utrecht, The Netherlands. *e-mail: A.Sluijs@uu.nl.

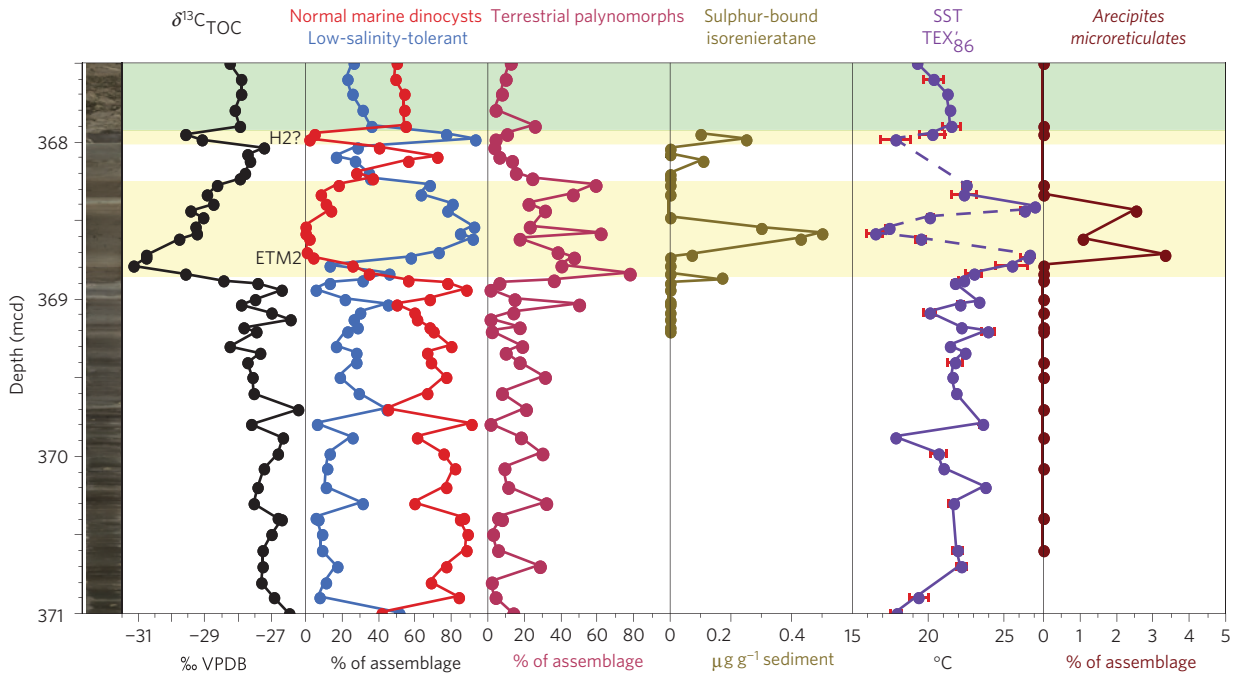

Figure 1 | Core photo and palynological and geochemical results across ETM2 of IODP Core 302-4A-27X, Lomonosov Ridge, Arctic Ocean. The yellow bars indicate intervals within the two negative CIEs. The green bar indicates an interval affected by severe drilling disturbance and/or caved material. The error bars for the TEX'_{86} data represent analytical errors, based on duplicate analyses. The open-marine dinoflagellate taxa include *Membranosphaera* spp., *Glaphyrocysta* spp., *Batiacasphaera* spp. and *Hystrichosphaeridium tubiferum*. The freshwater-tolerant taxa are dominantly *Senegalinium* spp. and *Cerodinium* spp.

This chemical fossil, which is below the detection limit outside this interval apart from one sample close to the onset of the CIE, is derived from the brown strain of photosynthetic green sulphur bacteria, which requires euxinic (anoxic and sulphidic) conditions[18]. The presence of isorenieratane indicates photic-zone euxinia developed in the Arctic Ocean during ETM2.

Terrestrial palynomorphs throughout the section are dominated by conifer pollen, such as *Metasequoia*-type (Taxodiaceae) and *Pinus* (pine), and include pollen types related to modern *Corylus* (hazel), *Quercus* (oak), *Carya* (pecan) and other types reflecting a warm-temperate and humid climate leading up to ETM2. Remarkably, within the interval 368.75–368.40 mcd, we recorded *Arecipites microreticulates* pollen, derived from Arecaceae (palms), described from the Eocene of Europe[19] (Fig. 1; Supplementary Fig. S3). Extant palms produce relatively few pollen grains and, thus, despite their low relative abundances (1–4% of the pollen assemblages), palms were probably a common constituent of the vegetation on land masses near the drill site. Apart from Palaeocene and Eocene assignments in Spitsbergen[20] and offshore Greenland[21], palms have not been reported north of 60° N in the Cenozoic of North America and Eurasia[22], making this their northernmost occurrence. Their appearance in the Arctic, hence, indicates substantial climate warming during ETM2.

At present, palms do not naturally occur in areas where the coldest month mean temperature (CMMT) is below 5 °C (refs 22, 23), and the most resistant species tolerate frost for only a few hours[24]. When grown at elevated CO_2 levels, palms are even less resilient, suggesting that the CMMT implied by the presence of their pollen in the Early Eocene was >8 °C (ref. 5). The palm pollen record suggests that this climatic threshold was exclusively passed during the warmest phase of ETM2. Moreover, it demonstrates that Arctic winter temperatures were dominantly above freezing during ETM2.

To reconstruct Arctic sea surface temperatures (SSTs) during ETM2, we used the palaeothermometer TEX'_{86} (ref. 7). TEX'_{86} is based on the distribution of crenarchaeotal membrane lipids and shows a linear correlation with mean annual SST in the modern ocean for temperatures between 5 and 30 °C with a calibration error of ~2 °C (Supplementary Fig. S2). In the Arctic, TEX'_{86}-based SST reconstructions may be skewed towards summer temperatures (Supplementary Information). Background Arctic SST values (below and just above ETM2, and above the supposed H2) average ~22 ± 1.4 °C. The variations within this interval may reflect SST changes, similar to those recorded just before ETM2 in the southeast Atlantic Ocean[2,3], but may also be associated with the varying influence of soil-derived lipids (Supplementary Information). During the onset of ETM2, TEX'_{86}-derived SSTs rose to 26–27 °C, indicating that SSTs warmed by 3–5 °C in the Arctic (Fig. 1).

Remarkably, within both the CIE of ETM2 at ~368.6 mcd and the smaller CIE at ~368.0 mcd, the TEX'_{86} record shows a marked drop. An interval of mid-hyperthermal cooling has never been reported. Moreover, palm pollen remains present in this interval. Hence, even though little temperature information is available from ETM2, factors other than SSTs probably influenced these TEX'_{86} values. In exactly this interval, maximum abundances of sulphur-bound isorenieratane and freshwater-tolerant dinoflagellates record periods of photic-zone euxinia and freshening surface waters (Fig. 1). Under such conditions, marine Crenarchaeota may reside at the deep, relatively cool chemocline, as seen in the modern Black Sea and during the deposition of various Pliocene and Pleistocene sapropels in the Eastern Mediterranean under 'Black Sea-like' conditions[25] (Supplementary Information). Potentially, hence, the lower TEX'_{86} values within ETM2 and the CIE at ~368.0 mcd may reflect temperatures at the chemocline rather than SSTs. Regardless of the exact cause, the anomalously low values may have masked the peak SSTs during the event, which may have been even higher than the 26–27 °C recorded for the lowermost part of ETM2 (Fig. 1).

The development of anoxic bottom waters and euxinic photic-zone conditions on Lomonosov Ridge during ETM2 were potentially caused by multiple factors. The recorded increase in

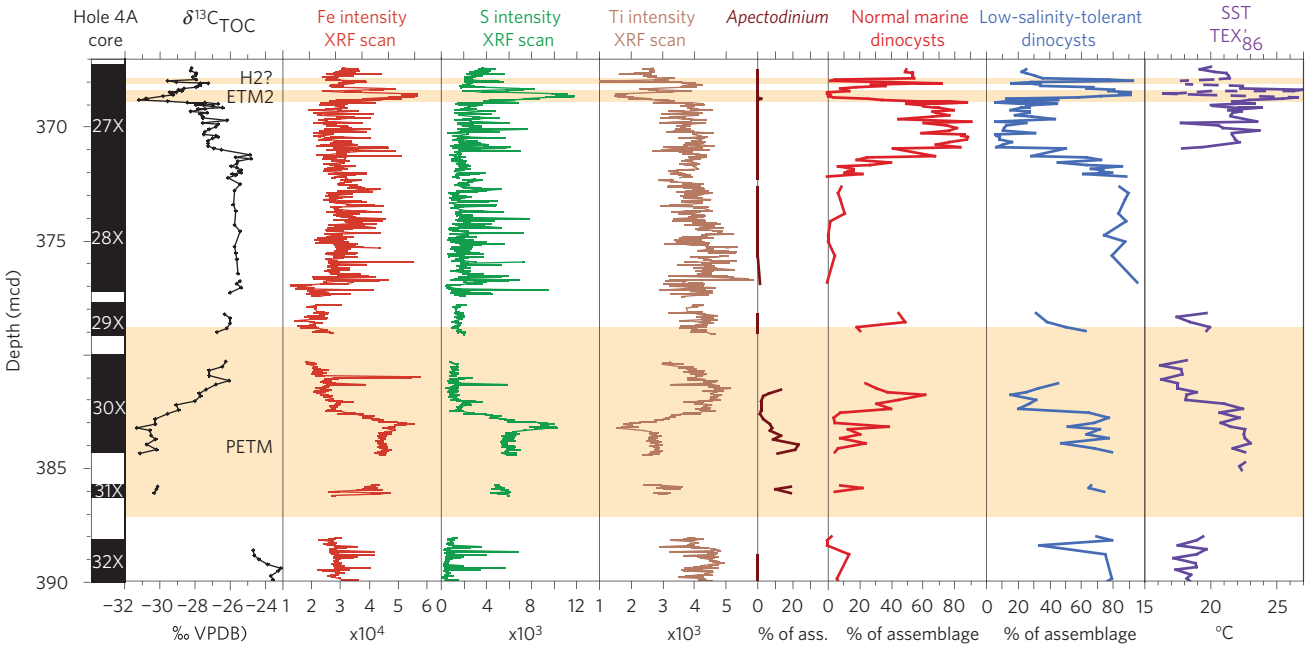

Figure 2 | Geochemical and palynological results across the latest Palaeocene and Early Eocene of IODP Hole 302-4A, Lomonosov Ridge, Arctic Ocean. PETM data are from ref. 7 ($\delta^{13}C_{TOC}$, TEX'_{86} and dinoflagellates) and ref. 8 (XRF).

freshwater input, greater nutrient load and warmer temperatures would all conspire to intensify stratification and reduce concentrations of dissolved O_2 in the water column. Given that photic-zone euxinia developed during maximum abundances of freshwater-tolerant dinocysts, rather than during the onset of ETM2 warming, an important factor was probably intense stratification owing to the influence of a fresh or brackish surface water lid.

A comparison of our ETM2 records to those generated previously from the PETM in the same core[7,8,11] shows that both events were associated with rapid warming, an increase in freshwater influx, increasing biological production rates and the development of water-column anoxia (Fig. 2). Furthermore, X-ray fluorescence (XRF) scanning shows identical patterns in elemental intensities (Fig. 2). For example, increases in Fe and S, for the PETM interpreted to reflect more reducing conditions at the sea floor[8], are also recorded for ETM2 and consistent with our evidence for stratified and anoxic conditions. These similarities corroborate the notion[2,4] that the ETM2 and the PETM shared a qualitatively similar climate response on land, and in shallow and deep oceans.

The dinocyst *Apectodinium* is generally absent throughout the ETM2 (Fig. 2), contrasting abundant occurrences within the Arctic PETM (ref. 7) and strata potentially of the ETM2 age reported from the Nordic seas[26,27]. The basal part of the ETM2, however, contains some *Apectodinium* spp., indicating that representatives of the genus migrated into the Arctic. The dominant species in PETM strata, *A. augustum*, is absent, excluding the possibility that the encountered *Apectodinium* specimens are reworked. Low salinities may not have been optimal for *Apectodinium* growth[28] and sea surface salinities potentially dropped below tolerable values during ETM2, also explaining the demise of the other open-marine taxa. This aspect, but also the persistence of open-marine dinoflagellate taxa during the PETM, implies that Arctic surface waters were fresher during ETM2 than during the PETM. Potentially, this could be associated with differences in regional basin geometry between ETM2 and the PETM. Alternatively, Arctic precipitation and runoff were even greater during ETM2 than during the PETM.

Background SSTs before the ETM2 are nearly 4 °C warmer than background temperatures around the PETM (ref. 7); in fact, SSTs were nearly as high as peak PETM temperatures (Fig. 2). This is consistent with a long-term warming trend during the Early Eocene as revealed by deep-sea records[1]. The magnitude of Arctic sea surface warming, however, was larger, suggesting that polar amplification of this long-term trend occurred even in the absence of ice–albedo feedbacks. TEX'_{86} records a 3–5 °C SST rise during ETM2. A core gap at the onset of the PETM at the same Arctic site may have led to an underestimation of PETM peak temperatures of up to 1 °C (Supplementary Information). Still, maximum TEX'_{86}-derived SSTs during ETM2 are ~3 °C warmer than those recorded for the PETM at the same site[7]. Moreover, palm pollen was recorded in ETM2 strata (Fig. 1), but not in the PETM. Collectively, we surmise that maximum Arctic temperatures during ETM2 were even warmer than during the PETM.

The CMMT of >8 °C provides the first estimate of Early Eocene Arctic winter temperatures and thereby a critical new constraint for testing Arctic temperature response to CO_2 forcing in fully coupled climate models. When forced with Early Eocene CO_2 concentrations and geography, these models produce CMMTs significantly below freezing[6]. Specifically, our results imply that some mechanism, probably through cloud feedbacks not incorporated in the models[29,30], substantially reduced Arctic winter cooling under high-CO_2 conditions. Depending on the climatic and greenhouse-gas concentration threshold at which such mechanisms become significant, they might comprise unforeseen positive feedbacks for future Arctic warming.

Methods

For palynological analyses, freeze-dried sediment was treated with 30% HCl and twice with 38% HF and sieved over a 15-μm nylon mesh. Residues were mounted on microscope slides, which were analysed at ×500 magnification.

All $\delta^{13}C$ analyses were done on freeze-dried samples with a Fison NA 1500 CNS analyser, connected to a Finnigan Delta Plus mass spectrometer. The analytical precision determined by replicate analyses was better than 0.1‰. All values are reported relative to the Vienna Pee Dee Belemnite (VPDB) standard.

For TEX'_{86} and S-bound isorenieratane analyses, powdered and freeze-dried sediments were extracted with a Dionex Accelerated Solvent Extractor using a 9:1 (v/v) mixture of dichloromethane and methanol. One aliquot of the extract was fractionated into apolar and polar fractions. Polar fractions, containing glycerol dialkyl glycerol tetraethers, were analysed using high-performance liquid chromatography/atmospheric pressure chemical ionization-mass spectrometry. Single-ion monitoring was used to quantify the abundance of the crenarchaeotal

lipids. Another aliquot of the total extract was desulphurized using Raney nickel and subsequently separated into polar and apolar fractions. Apolar fractions were hydrogenated using PtO_2/H_2 and analysed by gas chromatography (Agilent 6890) and gas chromatography/mass spectrometry (Thermofinnigan DSQ). Concentrations of isorenieratane were quantified by the addition of an internal standard (C_{22} ante-iso alkane) to the extract before desulphurization.

Elemental intensities at the surfaces of Cores 302-33X to -27X were measured using the X-Ray Fluorescence Core Scanner II at Bremen University with an Amptek detector.

Received 13 June 2009; accepted 28 September 2009; published online 25 October 2009

References

1. Zachos, J., Pagani, M., Sloan, L., Thomas, E. & Billups, K. Trends, rhythms, and aberrations in global climate 65 Ma to present. *Science* **292,** 686–693 (2001).
2. Lourens, L. J. *et al.* Astronomical pacing of late Palaeocene to early Eocene global warming events. *Nature* **435,** 1083–1087 (2005).
3. Stap, L., Sluijs, A., Thomas, E. & Lourens, L. J. Patterns and magnitude of deep sea carbonate dissolution during Eocene Thermal Maximum 2 and H2, Walvis Ridge, southeastern Atlantic Ocean. *Paleoceanography* **24,** doi:10.1029/2008PA001655 (2009).
4. Nicolo, M. J., Dickens, G. R., Hollis, C. J. & Zachos, J. C. Multiple early Eocene hyperthermals: Their sedimentary expression on the New Zealand continental margin and in the deep sea. *Geology* **35,** 699–702 (2007).
5. Royer, D. L., Osborne, C. P. & Beerling, D. High CO_2 increases the freezing sensitivity of plants: Implications for paleoclimatic reconstructions from fossil floras. *Geology* **30,** 963–966 (2000).
6. Shellito, C. J., Sloan, L. C. & Huber, M. Climate model sensitivity to atmospheric CO_2 levels in the Early-Middle Paleogene. *Palaeogeogr. Palaeoclimatol. Palaeoecol.* **193,** 113–123 (2003).
7. Sluijs, A. *et al.* Subtropical Arctic Ocean temperatures during the Palaeocene/Eocene thermal maximum. *Nature* **441,** 610–613 (2006).
8. Sluijs, A. *et al.* Arctic late Paleocene–early Eocene paleoenvironments with special emphasis on the Paleocene-Eocene thermal maximum (Lomonosov Ridge, Integrated Ocean Drilling Program Expedition 302). *Paleoceanography* **23,** PA1S11 (2008).
9. Cramer, B. S., Wright, J. D., Kent, D. V. & Aubry, M.-P. Orbital climate forcing of $\delta^{13}C$ excursions in the late Paleocene–early Eocene (chrons $C_{24}n$–$C_{25}n$). *Paleoceanography* doi:10.1029/2003PA000909 (2003).
10. Glebovsky, V. *et al.* Formation of the Eurasia Basin in the Arctic Ocean as inferred from geohistorical analysis of the anomalous magnetic field. *Geotectonics* **40,** 263–281 (2006).
11. Pagani, M. *et al.* Arctic hydrology during global warming at the Palaeocene-Eocene thermal maximum. *Nature* **442,** 671–675 (2006).
12. Stein, R., Boucsein, B. & Meyer, H. Anoxia and high primary production in the Paleogene central Arctic Ocean: First detailed records from Lomonosov Ridge. *Geophys. Res. Lett.* doi:10.1029/2006GL026776 (2006).
13. Schouten, S. *et al.* The Paleocene-Eocene carbon isotope excursion in higher plant organic matter: Differential fractionation of angiosperms and conifers in the Arctic. *Earth Planet. Sci. Lett.* **258,** 581–592 (2007).
14. Weijers, J. W. H., Schouten, S., Sluijs, A., Brinkhuis, H. & Sinninghe Damsté, J. S. Warm arctic continents during the Palaeocene-Eocene thermal maximum. *Earth Planet. Sci. Lett.* **261,** 230–238 (2007).
15. O'Regan, M. *et al.* Mid-Cenozoic Tectonic and Paleoenvironmental setting of the Central Arctic Ocean. *Paleoceanography* **23,** PA1S20 (2008).
16. Brinkhuis, H. *et al.* Episodic fresh surface waters in the Eocene Arctic Ocean. *Nature* **441,** 606–609 (2006).
17. Sluijs, A., Pross, J. & Brinkhuis, H. From greenhouse to icehouse; organic-walled dinoflagellate cysts as paleoenvironmental indicators in the Paleogene. *Earth Sci. Rev.* **68,** 281–315 (2005).
18. Sinninghe Damsté, J. S., Wakeham, S. G., Kohnen, M. E. L., Hayes, J. M. & de Leeuw, J. W. A 6,000-year sedimentary molecular record of chemocline excursions in the Black Sea. *Nature* **362,** 827–829 (1993).
19. Krutzsch, W. & Vanhoorne, R. Die Pollenflora von Epinois und Loksbergen in Belgien. *Palaeontographica Abt. B* **163,** 1–110 (1977).
20. Schweitzer, H.-J. Environment and climate in the early Tertiary of Spitsbergen. *Palaeogeogr. Palaeoclimatol. Palaeoecol.* **30,** 297–311 (1980).
21. Eldrett, J. S., Greenwood, D. R., Harding, I. C. & Huber, M. Increased seasonality through the Eocene to Oligocene transition in northern high latitudes. *Nature* **459,** 969–973 (2009).
22. Greenwood, D. R. & Wing, S. L. Eocene continental climates and latitudinal temperature gradients. *Geology* **23,** 1044–1048 (1995).
23. Van der Burgh, J. Some palms in the Miocene of the lower Rhenish Plain. *Rev. Palaeobotany Palynology* **40,** 359–374 (1984).
24. Larcher, W. & Winter, A. Frost susceptibility of palms: Experimental data and their interpretation. *Principes* **25,** 143–152 (1981).
25. Menzel, D., Hopmans, E. C., Schouten, S. & Sinninghe Damsté, J. S. Membrane tetraether lipids of planktonic Crenarchaeota in Pliocene sapropels of the eastern Mediterranean Sea. *Palaeogeogr. Palaeoclimatol. Palaeoecol.* **239,** 1–15 (2006).
26. Bujak, J. P. & Brinkhuis, H. in *Late Paleocene-Early Eocene Climatic and Biotic Events in the Marine and Terrestrial Records* (eds Aubry, M.-P., Lucas, S. G. & Berggren, W. A.) 277–295 (Columbia Univ. Press, 1998).
27. Sluijs, A. *et al.* Eustatic variations during the Paleocene-Eocene greenhouse world. *Paleoceanography* **23,** PA4216 (2008).
28. Sluijs, A. *et al.* Environmental precursors to light carbon input at the Paleocene/Eocene boundary. *Nature* **450,** 1218–1221 (2007).
29. Peters, R. B. & Sloan, L. C. High concentrations of greenhouse gases and polar stratospheric clouds: A possible solution to high-latitude faunal migration at the latest Paleocene thermal maximum. *Geology* **28,** 979–982 (2000).
30. Abbot, D. S., Huber, M., Bousquet, G. & Walker, C. C. High-CO_2 cloud radiative forcing feedback over both land and ocean in a global climate model. *Geophys. Res. Lett.* **36,** L05702 (2009).

Acknowledgements

This research used samples and data provided by the Integrated Ocean Drilling Program (IODP). Financial support for this research was provided by the Netherlands Organisation for Scientific Research to A.S. (NWO-Veni grant 863.07.001), S.S. (NWO-Vici grant), P.L.S., F.S., J.S.D. and H.B., and by the Deutsche Forschungsgemeinschaft (DFG) to U.R. We thank G. Harrington (University of Birmingham) and M. Harley (Royal Botanical Gardens, Kew) for confirming the identification of *Arecipites* pollen, J. van der Burgh (Utrecht University), the IODP Expedition 302 Scientific Party and Urbino Summer School in Palaeoclimatology Instructors for discussions, and L. Bik, E. C. Hopmans, A. Mets, J. van Tongeren and N. Welters for technical support.

Author contributions

A.S., S.S., U.R. and H.B. designed the research, A.S., T.H.D. and H.B sampled the core, A.S. and G.J.R. generated $\delta^{13}C_{TOC}$ data, A.S. and H.B. analysed dinoflagellate cyst assemblages, T.H.D. analysed the terrestrial palynomorphs, S.S., P.L.S., F.S. and J.S.D. carried out sulphur-bound isorenieratane and TEX'_{86} analyses, J.H.K. calculated the revised TEX'_{86} calibration and U.R. carried out XRF core scanning. All authors contributed to data interpretation. A.S. and S.S. wrote the paper with input from all authors.

Additional information

Supplementary information accompanies this paper on www.nature.com/naturegeoscience. Reprints and permissions information is available online at http://npg.nature.com/reprintsandpermissions. Correspondence and requests for materials should be addressed to A.S.